

Enabling Exoplanet Demographics Studies with Standardized Exoplanet Survey Meta-Data

PREPARED BY THE EXOPAG SCIENCE INTEREST GROUP (SIG) #2 ON EXOPLANET DEMOGRAPHICS,
JESSIE L. CHRISTIANSEN,¹ DAVID P. BENNETT,^{2,3} ALAN P. BOSS,⁴ STEVE BRYSON,⁵
JENNIFER A. BURT,⁶ RACHEL B. FERNANDES,⁷ TODD J. HENRY,⁸ WEI-CHUN JAO,⁹
SAMSON A. JOHNSON,^{10,6} MICHAEL R. MEYER,¹¹ GIJS D. MULDER,^{12,13} SUSAN E. MULLALLY,¹⁴
ERIC L. NIELSEN,¹⁵ ILARIA PASCUCCI,⁷ JOSHUA PEPPER,¹⁶ PETER PLAVCHAN,¹⁷ DARIN RAGOZZINE,¹⁸
LEE J. ROSENTHAL,¹⁹ AND ELIOT HALLEY VRIJMOET^{9,8}

¹*Caltech/IPAC-NASA Exoplanet Science Institute, Pasadena, CA 91125, USA*

²*Laboratory for Exoplanets and Stellar Astrophysics, NASA Goddard Space Flight Center, Greenbelt, MD 20771, USA*

³*Department of Astronomy, University of Maryland, College Park, MD 20742, USA*

⁴*Earth & Planets Laboratory, Carnegie Institution for Science, 5241 Broad Branch Road, NW, Washington, DC 20015-1305*

⁵*NASA Ames Research Center, Moffett Field, CA 94035, USA*

⁶*Jet Propulsion Laboratory, California Institute of Technology, 4800 Oak Grove Drive, Pasadena, CA 91109, USA*

⁷*Lunar and Planetary Laboratory, The University of Arizona, Tucson, AZ 85721, USA*

⁸*RECONS Institute, Chambersburg, PA 17201, USA*

⁹*Department of Physics and Astronomy, Georgia State University, Atlanta, GA 30303, USA*

¹⁰*Department of Astronomy, The Ohio State University, 140 West 18th Avenue, Columbus OH 43210, USA*

¹¹*Department of Astronomy, University of Michigan, Ann Arbor, MI USA 48109*

¹²*Facultad de Ingeniería y Ciencias, Universidad Adolfo Ibáñez, Av. Diagonal las Torres 2640, Peñalolén, Santiago, Chile*

¹³*Millennium Institute for Astrophysics, Chile*

¹⁴*Space Telescope Science Institute, 3700 San Martin Drive, Baltimore, MD 21218, USA*

¹⁵*Kavli Institute for Particle Astrophysics and Cosmology, Stanford University, Stanford, CA 94305, USA*

¹⁶*Department of Physics, Lehigh University, 16 Memorial Drive East, Bethlehem, PA 18015, USA*

¹⁷*Department of Physics and Astronomy, George Mason University, Fairfax, VA 22030, USA*

¹⁸*Department of Physics & Astronomy, N283 ESC, Brigham Young University, Provo, UT 84602, USA*

¹⁹*MIT Lincoln Laboratory, 244 Wood Street, Lexington, MA 02421-6426*

1. EXECUTIVE SUMMARY

Goal 1 of the National Academies of Science, Engineering and Mathematics Exoplanet Science Strategy¹, which was endorsed by the Decadal Survey on Astronomy and Astrophysics 2020, is “to understand the formation and evolution of planetary systems as products of the process of star formation, and characterize and explain the diversity of planetary system architectures, planetary compositions, and planetary environments produced by these processes”, with the finding that “Current knowledge of the demographics and characteristics of planets and their systems is substantially

Corresponding author: Jessie Christiansen
christia@ipac.caltech.edu

¹ <https://www.nap.edu/catalog/25187/exoplanet-science-strategy>

incomplete.” One significant roadblock to our ongoing efforts to improve our demographics analyses is the lack of comprehensive meta-data accompanying published exoplanet surveys. The Exoplanet Program Analysis Group (ExoPAG) Science Interest Group #2: Exoplanet Demographics has prepared this document to provide guidance to survey architects, authors, referees and funding agencies as to the most valuable such data products for five different exoplanet detection techniques—transit, radial velocity, direct imaging, microlensing and astrometry. We find that making these additional data easily available would greatly enhance the community’s ability to perform robust, reproducible demographics analyses, and make progress on achieving the most important goals identified by the exoplanet and wider astronomical community.

2. INTRODUCTION

The field of exoplanets has now firmly moved from detection and characterization of individual objects and systems to characterization of entire populations of objects and systems. By studying the demographics of exoplanetary systems, we learn more about the physical mechanisms that drive their formation (e.g. Mordasini et al. 2016; Lee & Chiang 2016; Jin & Mordasini 2018), migration (e.g. Dawson & Murray-Clay 2013; Yu et al. 2021), and evolution (e.g. Owen & Wu 2017; Ginzburg et al. 2018).

The exoplanet detection techniques that have provided sufficient detections for population studies cover very different areas of parameter space in both stellar and planet properties. Observational biases push the different detection techniques toward different populations of stellar hosts (across properties such as distance, mass, age, activity, stellar multiplicity), and different populations of planets (across such properties as radius, mass, orbital period, planet multiplicity, and proximity to resonance). For example, transit and radial velocity surveys are most sensitive to close-in planets (<1 au), microlensing surveys and radial velocity to planets around the ice line (~ 1 – 10 au), and direct imaging surveys to distant planets (>10 au).

Although the detection techniques probe different pieces of parameter space, together they produce a broad census of planet populations. Exploiting this coverage to produce a comprehensive understanding of planet demographics is a crucial input to the planning and design of future NASA mission prioritized by the 2020 Decadal Survey on Astronomy and Astrophysics², and to achieving NASA’s strategic objectives of “discovering the secrets of the universe” and “searching for life elsewhere”³. The challenge is to stitch these different pieces together to provide a robust, overarching understanding of the demographics of planets and planetary systems. Such a process requires disentangling the stellar and planet population biases inherent to each technique, as well as correcting for the detection sensitivity and reliability of each individual survey. In addition, survey results are often reported in terms of planet occurrence rates, but these rates depend on assumptions made about the underlying planet population, and these assumptions are not always consistent across detection methods and surveys, leading to diverging results.

There have been several notable attempts to combine demographics results from multiple detection techniques (e.g. Clanton & Gaudi 2014, 2016; Kunimoto & Bryson 2021). Other studies have compared the results of different detection techniques without attempting to fit them with a single planet population. Examples include Fig. 2 of Pascucci et al. (2018), which compares transit and

² <https://www.nationalacademies.org/our-work/decadal-survey-on-astronomy-and-astrophysics-2020-astro2020>

³ https://science.nasa.gov/science-red/s3fs-public/files/nasa_2018_strategic_plan_0.pdf

microlensing results, Fig. 2 of [Fernandes et al. \(2019\)](#), which compares transit and radial velocity results, Fig. 8 of [Nielsen et al. \(2019\)](#), which compares radial velocity and direct imaging results, and Figures 9 and 10 of [Fulton et al. \(2021\)](#) which compare radial velocity vs. direct imaging and vs. microlensing. As yet, there have been few wide-ranging analyses that take advantage of the survey data that are currently available.

The difficulty in moving forward with synthesizing results from multiple detection techniques is typically that these survey data are not accompanied with the meta-data necessary to be reliably incorporated with other surveys. This includes, for instance, information about the surveys themselves, the stars observed, and the criteria for planets detected. There are certainly hurdles to making these data available: identifying the types and formats of the ancillary information needed; performing the work to create the data products, and making them readily accessible once published. However, there is significant benefit to undertaking this effort, including a substantial increase in the use, visibility, and citations of the accompanying survey data. For example, the NASA *Kepler* mission provided a wealth of additional information characterizing the survey⁴ (e.g. [Thompson et al. 2018](#); [Christiansen et al. 2020](#)), allowing many teams across the community to perform their own independent investigations of the data (e.g. [Fernandes et al. 2019](#); [Mulders et al. 2015, 2018](#); [Hsu et al. 2019](#); [Zink & Hansen 2019](#)).

Another challenge with missing meta-data arises when moving beyond demographics of individual planets to understanding the demographics of planetary system architectures, where correlations between planets within a particular system are of high scientific value but can often be biased by the survey or analysis technique (e.g. [Zink et al. 2021](#)). As we continue to move into a regime where planetary systems have different planets detected by different techniques, improved understanding of survey properties with respect to multi-planet systems will be crucial.

The goal of this document is to lay out, in some detail, the necessary ancillary information for five different exoplanet detection techniques—transit, radial velocity, direct imaging, microlensing, and astrometry—that could be published alongside exoplanet survey data to ensure those data are maximally useful to the demographics community. In particular, we find that intermediate data products generated as part of occurrence rate calculations are often not published, but are instrumental in combining data both from surveys using the same detection technique, and across multiple detection techniques. As such, we find that making these additional data easily available would greatly enhance the community’s ability to perform robust, reproducible occurrence rate calculations.

The audience for this document includes, but is not limited to:

- Authors publishing exoplanet survey data;
- Referees for journals publishing exoplanet survey data;
- Funding agencies considering proposals that would fund the collection, analysis, and publication of exoplanet survey data

This document was created by the NASA Exoplanet Program Analysis Group (ExoPAG) Science Interest Group (SIG) on Exoplanet Demographics. It includes input from astronomers publishing exoplanet survey data across all the major detection techniques, and those actively working in exoplanet

⁴ [NASA Exoplanet Archive: Kepler Completeness and Reliability Products](#)

demographics. In assembling these recommendations, we identified two ‘tiers’ of data products. We find that availability of **Tier I** data products would enable rudimentary incorporation of published exoplanet survey data into other analyses, using either the same or different detection techniques. Tier I products are those which are typically readily at hand, and are required for someone to be able to make some attempt to integrate the data in their analysis. We find that availability of **Tier II** data products would greatly enhance the community’s ability to incorporate published exoplanet survey data into their analyses, using either the same or different detection techniques. Tier II data products are those which may require more effort to produce or archive due to computational and data volume limitations, but would enable a robust inclusion and maximum usefulness of the published data set. In addition, for each detection technique we highlight in bold the data product that would be most useful for incorporating the survey results in demographics analyses, in order to help the community prioritize their resources.

An illustrative example is the survey detection completeness: while the survey-averaged completeness as described in the Tier I data products allows for a reproduction of survey results or a re-analysis with a different methodology, the per-star completeness described in the Tier II data products allows for new analyses of specific sub-samples of stars within the survey. The latter provides the community much greater flexibility in, for instance, combining targets from different surveys and accounting for target overlaps between surveys. In addition to the tiers, we identify three data ‘types’, for ease of categorizing: data pertaining to the **stellar sample**, data pertaining to the **survey properties**, and data pertaining to the **planet catalog**.

One driving philosophy in defining the products below is the goal that they are kept as close to the ‘observable’ units as possible. For instance, each detection technique measures a different property of the exoplanet size: transits measure the planet radius (or, more correctly, the planet-to-star radius ratio); radial velocity measures the planet mass projected along the line of sight with respect to the stellar mass; microlensing and astrometry measure the planet-to-star mass ratio; and direct imaging measures the planet luminosity in a given waveband. Each of these planet properties can be mapped onto the others through a variety of models and relations, however different models and relations may give different results and some of these relations are probabilistic in nature, (e.g. [Wolfgang et al. 2016](#)), and groups will have preferences as to the models and relations they wish to employ. We find that publication of survey and accompanying data in these native units would allow for future refinement of models and relations as our understanding improves. In addition, where authors have transformed their observables into other properties, we find that supply of the models and/or assumptions used in the transformation allows for a more extensive utility of the data set. Keeping the data in their native observable units also more naturally allows for updates as stellar parameters, such as the age, distance, or mass, are updated.

A second driving philosophy is that of reproducibility: survey data are often published without sufficient accompanying data for their demographics results to be reproduced by independent teams. Part of the motivation for this document is to enable authors to provide the data required for the demographics community to reproduce their results. In that vein, we find that the public availability of analysis codes used in publications greatly improves their reproducibility. Finally, we find that providing the described data products in machine-readable format (as compared to figures from which the relevant data would need to be extracted) is also crucial for allowing reproducibility.

For each detection technique below, we provide below the Tier I and Tier II data products for the three data types. We find that there is significant new exoplanet science to be explored if these data are more readily available. We also invite feedback on these lists, particularly if there is anything we have overlooked.

3. TRANSITS

The transit method measures the ratio of the planetary radius to the stellar radius, as well as the orbital period of exoplanets. Because the transit probability for an individual system is low, transit surveys are typically designed to monitor large number of stars in order to detect exoplanets. The detection probability of a transiting planet is a strong function of its orbital period and planet radius, ranging from $\sim 10\%$ for hot Jupiters to below a fraction of a percent for (super-)Earth-sized planets in the habitable zones around sun-like stars (see, e.g. [Borucki & Summers 1984](#)).

To do population studies, that measure either the intrinsic occurrence of planets or the dependence of occurrence on planet properties, the planet detection efficiency—the fraction of planets at a given detection threshold successfully recovered—has to be estimated. This can be done approximately by using a transit signal-to-noise threshold, above which one assumes 100% detection efficiency (e.g. [Howard et al. 2012](#)), or empirically by using injection-recovery tests to measure real pipeline performance (e.g. [Thompson et al. 2018](#); [Christiansen et al. 2020](#)).

Ground-based and space-based transit surveys employ different observation strategies and probe different parts of exoplanet parameter space. Space-based observatories allow for continuous monitoring of large groups of stars at high sensitivity. For example, the *Kepler* spacecraft monitored almost 200,000 stars for transiting planets as small as Earth with periods up to a year, enabling precise estimates of the occurrence of planets and fraction of stars with planetary systems within 1 au (e.g. [Mulders et al. 2018](#); [Hsu et al. 2019](#); [He et al. 2019](#)). A similar dataset with over 200,000 stars from the *K2* mission is also available ([Zink et al. 2021](#)). The Transiting Exoplanet Survey Satellite (TESS, [Ricker et al. 2015](#)) is significantly increasing the number of stars with continuous, high-precision time series photometry with millions of light curves from an all sky survey ([Kunimoto et al. 2021a](#)) and identifying thousands of transiting planet candidates (e.g. [Kunimoto et al. 2021b](#)).

Ground-based observatories are limited in the time and number of stars they can monitor. They have been very efficient in discovering hot Jupiters, or targeting specific sub-sets of stars such as M dwarfs to look for habitable zone planets ([Nutzman & Charbonneau 2008](#); [Jehin et al. 2011](#)), but have been less proficient in providing uniform catalogues for planet occurrence rate studies.

Given the large number of stars in transit surveys, the survey detection efficiency is often presented as a *survey-averaged completeness* that can be used to make exoplanet population inferences across the stellar sample. Because planet occurrence rates do vary with stellar properties ([Howard et al. 2012](#); [Mulders et al. 2015](#)), a description of the stellar sample is needed to place these inferences in context with those of other surveys that target different groups of stars, such as microlensing surveys (e.g. [Suzuki et al. 2016](#); [Pascucci et al. 2018](#)). A description of the stellar sample is therefore also included in the Tier I data products.

The Tier II data products include the per-star detection efficiency. Providing this data could enable additional science cases such as investigating stellar dependencies in the planet population, and is especially useful for synergies with other detection methods.

3.1. Tier I Data Products

1. Stellar sample properties

- (a) Description of stellar sample that was searched. This includes target selection criteria and number of stars in the survey.
- (b) Provenance of stellar parameters, in case multiple catalogues are available.
- (c) Description of the properties of stars that were removed from the parent sample (e.g. possible evolved star or binary, lack of high quality data, etc.)

2. Survey parameters

- (a) Description of criteria used for signal detection and planet candidate vetting (SNR threshold, minimum number of transits required, etc.)
- (b) Survey-level summary of observational coverage such as a window function, or duty cycle and time coverage
- (c) Description of treatment of planet multiplicity. Procedure to search the lightcurve for additional transit signals.
- (d) Detection and vetting efficiency of survey; either estimated or based on injection-recovery tests.
- (e) Treatment for stellar binarity and flux dilution/contamination from nearby or background stars.

3. Planet catalog properties

- (a) Properties of each host star: mass, radius, effective temperature, and surface gravity. If available, the limb darkening coefficients used for deriving the planet to star radii from the transit depth.
- (b) Observed properties of each planet candidate: orbital period, transit depth (or planet-to-star radius ratio), and transit duration. If available, estimates of the impact parameter or orbital eccentricity.
- (c) Sample reliability (measured or estimated, or assumptions made), including both the astrophysical false positive probability and the instrumental false alarm rate.

3.2. Tier II Data Products

1. Stellar sample properties

- (a) Full list of surveyed stars with fundamental properties (identifier, radius, mass, effective temperature, limb darkening coefficients, age estimates, etc.) and their provenance.
- (b) Stellar properties used in defining the survey sample, if those are updated during or after the survey.

2. Survey properties

- (a) Per-target detection efficiency, either estimated from a detection model or as empirically measured with injection-recovery tests. In terms of orbital period and planet-to star radius ratio (or depth). Alternatively, the per-target detection efficiency can also be expressed in terms of the measured signal-to-noise (or MES) and the number of transits observed.

- (b) Per-target observing window length including gaps, or 1-sigma depth functions
- (c) The detection efficiency of additional planets in the system.

3. Planet catalog properties

- (a) Simulated data sets. Inputs and results of a large suite of simulated data sets based on the pipeline used to generate the planet catalog. Simulated data sets might be based on an astrophysical model plus a model for the noise, or make use of alternative strategies such as scrambling or inverting the data.

4. RADIAL VELOCITIES

Doppler surveys operate by measuring the change in a star’s velocity between numerous, high resolution, spectroscopic observations, and can measure the orbital period, eccentricity, and minimum mass of planets orbiting the target star. Because radial velocity (hereafter, RV) detections do not require an exoplanet to transit its host star, this method is sensitive to a wider range of orbital configurations and to longer period planets than the transit surveys described above. A planet’s RV amplitude is a function of its orbital period, mass, eccentricity and inclination – as such massive, short period, planets seen edge-on are generally easier to detect while low mass, long period planets are more challenging.

Current RV exoplanet surveys tend to target older stars when performing uninformed planet searches, as stars older than about 1 Gyr are much more RV-quiet than their younger counterparts. RV sensitivity to a planet is determined by the number of RV measurements, the single point measurement precision of these measurements, the ratio of the observational baseline to the planet’s orbital period, the cadence and windowing of the observations, instrumental precision and systematics, and stellar variability created by phenomena such as granulation, magnetic activity and spot rotation. Quantifying the Doppler sensitivity for a particular star given an existing RV data set is generally accomplished via the use of injection and recovery analyses.⁵

4.1. Tier I Data Products

1. Stellar sample properties

- (a) Catalog of target stars including information on their spectral types, magnitudes, and masses
- (b) Total time span of observations for each target star, including start and end dates
- (c) Number of RV epochs for each target star
- (d) Median RV precision for each star’s RV data set

2. Survey parameters

- (a) Time baseline of survey, start and end
- (b) Average number of observations per survey target star

⁵ For a detailed discussion of such studies and links to an open source python package for running this type of analysis see, e.g., [Rosenthal et al. \(2021\)](#).

- (c) Estimated survey average detection efficiency as a function of RV semi-amplitude (K) and orbital period derived from injection recovery tests⁶

3. Planet catalog properties

- (a) Properties of each planet candidate: orbital period, RV semi-amplitude, orbital eccentricity and longitude of periastron ω (if used), time of conjunction of periastron (if used), $m\sin i$, and some quantification of the signal strength (FAP, ΔBIC , etc.)

4.2. Tier II Data Products

1. Stellar sample properties

- (a) Target selection function (for instance, any cuts applied on rotational velocity, apparent magnitude, spectral type, stellar activity, stellar multiplicity, etc)
- (b) Properties of each host star: apparent magnitude, spectral type, effective temperature, coordinates, mass, radius, distance; in addition, any of the following if known: activity indicators, rotation period, age, metallicity, multiplicity, rotational velocity
- (c) Median single measurement precision for each target star
- (d) **RV time-series for each target star, including BJD times of observation, RV, RV uncertainty (due to photon + instrument uncertainties), and SNR in a representative echelle order.** Or if data is still proprietary then the above list without the actual RVs, but still including the BJD times of observation, RV uncertainty, and SNR.
- (e) Details of stellar activity related modeling, if performed in planet detection:
 - Activity or ancillary spectroscopic indicator time-series:
 - Canonical activity indices such as S-index, H-alpha, etc, if used
 - CCF bisector time-series, as a whole, and/or line-by-line depending on RV extraction methodology, if used
 - Line-by-line flux-depth time-series if utilized
 - Order-by-order chromatic RV measurements if utilized
 - Other activity indicator time-series
 - Specification of any kernel used for activity temporal modeling, including Gaussian Process (GP) hyperparameters such as spot lifetime, rotation period, GP amplitude, smoothness, etc.
 - Details on any photometry or other time series data used to estimate the star's rotation period, oscillation/granulation strength, etc, if these parameters were used in the planet search process.

2. Survey parameters

- (a) Details of methodology, priors for planet fit parameters, etc.

⁶ Given the way most existing RV surveys are carried out, there is no guarantee that the Doppler sensitivity will be the same even for stars of the same spectral type and magnitude. As RV observations require targeting each star individually, stars generally end up with varying numbers of observations and levels of RV precision depending on the science goals of the survey.

- (b) Telescope(s) and spectrograph(s) used, including spectrograph configuration(s) if applicable
- (c) Any specialized cadence or observing constraints (e.g. bright time only)
- (d) Per-star 50% detection probability as a function of $m_{\text{sin}i}$ and orbital period
- (e) Recovery results for each period and K combination injected into the RV data, in a tabular format
- (f) Notes on any targets that were added or dropped during the survey, or targets for which the priority of observation planning was changed mid-survey due to evidence of a planet candidate, etc. In the ideal case, this would take the form of an additional column in the RV time series that would denote why each observation was triggered (e.g., part of a given survey’s algorithmic observations, part of a small proposal to get extra observations for a few targets, because the observing team gave it a priority increase, etc.).

3. Planet catalog properties

- (a) Detailed planet orbital information: period, semi-amplitude, eccentricity and longitude of periastron ω (if used), mean anomaly, and some quantification of the signal strength (e.g. FAP or ΔBIC), etc.
- (b) Posterior samples, annotated with log prior and log likelihoods separately, so that other authors can reweight the sample to account for different priors. Particularly, for low SNR detections where uncertainties can be large and non-Gaussian.
- (c) Check on whether the signal’s period also appears in the star’s activity time series
- (d) Check on whether the signal’s period could be due to survey design (e.g. aliasing, window function, etc.)

5. DIRECT IMAGING

Direct imaging requires overcoming the extreme contrast ratios and small angular separation between planet and host star. Advances in adaptive optics on large ground-based telescopes and coronagraphy have made way for the detection of exoplanets at small angular separation (e.g. [Macintosh et al. 2018](#); [Beuzit et al. 2019](#)). Most direct imaging exoplanet surveys target young planets in the infrared, as young planets are hotter and brighter, and present a more favorable contrast ratio to their host star ([Bowler 2016](#)). More advanced imaging instrumentation on large telescopes, coupled with large target lists of young, nearby stars have enabled direct measurements of the demographics of young, giant planets ($\gtrsim 1M_{Jup}$) at wider separations ($\sim 10\text{-}100$ au) around nearby stars (e.g. [Nielsen et al. 2019](#); [Vigan et al. 2021](#)).

Imaging observations of a given star are characterized by a contrast curve, the minimum flux of a planet that is detectable as a function of projected separation from the star. Demographic studies from imaging data use these contrast curves and target properties to translate the observing sensitivity into a completeness to planets. Theoretical models (e.g. [Baraffe et al. 2003](#); [Marley et al. 2021](#)) provide spectra of exoplanets as a function of planet mass and system age. Then, given the age and apparent magnitude of each target star, these theoretical models are used to convert the contrast curve from flux ratio units (in a given passband) into planet mass. Typically, projected separation is also converted to orbital semi-major axis by marginalizing over possible orbital parameters. Given

the limited number of young, nearby stars in the sky (for example, those in nearby moving groups, [Gagné & Faherty 2018](#)), different demographic studies often have overlapping target lists.

5.1. Tier I Data Products

1. Stellar sample properties

- (a) Description of stellar sample that was searched, including target selection criteria and number of stars in survey
- (b) Properties of each target star: age, distance, magnitude in the observing band
- (c) Provenance of stellar parameters

2. Survey properties

- (a) Description of the criteria used for detection
- (b) Description of image processing method, and characterization of any bias introduced
- (c) Contrast curves (in units of delta-magnitude as a function of projected separation in arcseconds) for each observation of each target star (with and without planets). If azimuthally-collapsed 1D contrast curves are produced, the 2D images should be preserved
- (d) Noise estimation method

3. Planet catalog

- (a) Observed properties of each companion: delta-magnitude, epoch of detection, projected separation at detection, and position angle
- (b) Theoretical model used to convert planet luminosity to planet mass
- (c) False alarm probability or other method/s of characterizing sensitivity

5.2. Tier II Data Products

1. Stellar sample properties

- (a) Probability distributions for stellar age and mass for each star, if generated.

2. Survey properties

- (a) 2D plots (and underlying data) showing fractional completeness to planets around each star as a function of semi-major axis and planet mass (depth of search plots, or "tongue plots")
- (b) Raw and processed images after completion of a given demographics study to enable reanalysis with new techniques.

6. MICROLENSING

The microlensing technique enables the measurement of the planet-host mass ratio, q , and the projected orbital separation of a planet relative to the size of the Einstein ring radius of the host star, $s = a_{\perp}/R_E$ ([Gaudi 2012](#)). Microlensing events are inherently rare, requiring the near perfect alignment of a lensing system with a background source star. As such, microlensing surveys monitor

the Galactic Bulge where the event rate peaks with a large number of potential sources and planetary lens systems. The primary advantage of the microlensing method is its sensitivity to low-mass planets (Bennett & Rhie 1996) in relatively wide orbits. The microlensing method is most sensitive to planets orbiting at separations within a factor of two of the Einstein radius, which is typically 2-3 AU (Gould & Loeb 1992). Microlensing’s unique sensitivity to low-mass planets in wider orbits was the rationale for the selection of an exoplanet microlensing survey as one of the main goals of the top ranked *Nancy Grace Roman Space Telescope* (formerly *WFIRST*) by the Astro2010 decadal survey.

With one notable exception (Nucita et al. 2018), all planetary microlensing events have been detected toward the Galactic bulge, including the discoveries by the Optical Gravitational Lens Experiment (OGLE), the Microlensing Observations in Astrophysics group (MOA), and the Korean Microlensing Telescope Network (KMTNet). The *Roman* Galactic Bulge Time Domain Survey (Penny et al. 2019) will also monitor the central Galactic bulge in order to carry out its exoplanet microlensing survey. As the distribution of lens systems studied by these surveys extends from near the Earth to the Galactic center, microlensing can detect planets throughout the Galaxy. The parameters measured directly from virtually all planetary microlensing events are q and s , the mass ratio and separation in Einstein radius units. Some have argued that the mass ratio is more fundamental than the planet mass (Pascucci et al. 2018), and for microlensing events it is more sensible to characterize planetary systems with planetary mass ratios and host star masses, instead of the masses of the host and the planets. The determination of the host star masses and their distance from us does not automatically come from the light curve models and relies upon additional observations and/or the measurement of subtle light curve features as we discuss in Section 6.1.

The characteristic timescale of a microlensing event, t_E , for a stellar lens is typically tens of days, but ranges from four to > 100 days for known planetary microlensing events. Light curve perturbations due to planets have a duration that can be less than a few hours.. A balance must be made between observation cadence and survey area to detect as many events as possible but maintain a cadence to characterize planetary anomalies. Microlensing exoplanet searches often employ auxiliary observations targeted at events that showed early potential of exhibiting a planetary signal. If these auxiliary observations are scheduled based on a possible planetary signal, this has the potential to bias the results if the triggering of these auxiliary observations is not properly accounted for in the statistical analyses. However, the selection of high magnification events (Gould et al. 2010) or bright source stars (Gaudi et al. 2002; Cassan et al. 2012) because of their high sensitivity to exoplanet signals does not cause such a bias. Since follow-up observers are strongly tempted to observe events with possible planetary signals in progress, it is helpful to define a protocol to ensure a well defined statistical sample in advance (Yee et al. 2015).

High cadence microlensing surveys with wide field telescopes (Suzuki et al. 2016; Poleski et al. 2021) can survey many more microlensing events than follow-up programs and therefore have a higher planetary signal detection rate. So, we expect that most future exoplanet microlensing demographics papers will be based on high cadence surveys. Nevertheless, data taken in response to the identification of a possible planetary signal can still be used to more precisely determine the lens system properties, as long as the originally scheduled survey observations are sufficient to establish that the possible planetary signal is above the detection threshold (Suzuki et al. 2016).

The exoplanet microlensing demographics papers to date (Gaudi et al. 2002; Sumi et al. 2010; Gould et al. 2010; Cassan et al. 2012; Suzuki et al. 2016; Poleski et al. 2021) have all used the

planet-star mass ratio, q , and the separation on the plane of the sky in Einstein radius units, s , to characterize the planetary systems. This is done because, this information comes directly from the light curve model for virtually all events, although there are some events with degenerate light curve models, particularly the close-wide degeneracy that yields nearly identical light curves for most high magnification events with the substitution $s \leftrightarrow 1/s$.

One of the main challenges for the microlensing method is determine the masses and distances of the planetary systems discovered with this method. This would enable a more direct comparison to the demographics from radial velocity and direct imaging surveys, although some progress can be made without mass and distance measurements (e.g., Clanton & Gaudi 2016). The next major advance in exoplanet microlensing is the *Nancy Grace Roman Space Telescope* (*Roman*) Galactic Bulge Time Domain Survey (Penny et al. 2019). *Roman* will produce a statistical sample of planets comparable to *Kepler*'s results from $\lesssim 1$ au, but in a complementary region of parameter space from 1 to $\gtrsim 10$ au. In addition to a much larger sample of microlens planetary systems, *Roman* will determine the masses and distances for more than half the planetary systems that it discovers, using the methods described in the next section.

6.1. Microlens Mass and Distance Measurement Methods

There are three methods that yield mass-distance relations for microlensing events: measurement of the angular Einstein radius, θ_E , measurement of the microlensing parallax parameter, π_E , and the brightness of the source star. Figure 1 shows these mass distance relations for planetary microlensing event MOA-2009-BLG-319 (although π_E was not actually measured for this event). Any two of these measurements can yield a mass and distance solution, and all three of them give redundant constraints that can be used to check for systematic errors.

MOA-2009-BLG-319 M_L, D_L Constraints

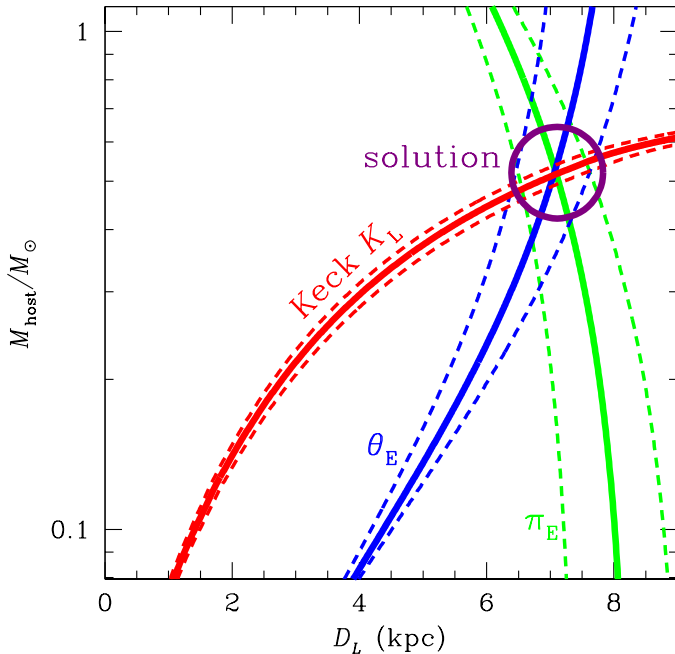


Figure 1. Three mass-distance relations are plotted for planetary microlensing event MOA-2009-BLG-319. The constraints from the measured angular Einstein radius, θ_E , are shown in blue; the Keck K-band lens brightness measurement, K_L is shown in red, and the microlensing parallax, π_E , constraint is shown in green (although π_E was not actually measured for this event). The dashed lines are $1\text{-}\sigma$ error bars. The intersection of these curves yields the lens system mass and distance, and the planet-star mass ratio determined from the microlensing light curve gives the individual star and planet masses.

The angular Einstein radius can be determined from finite source effects that are measured for most planetary microlensing events, particularly those with low-mass planets via $\theta_E = \theta_* t_E / t_*$, where θ_* is

the angular radius of the source star, which is determined from its extinction corrected magnitude and color. The microlensing parallax parameter, π_E , is the inverse of the length of the Einstein radius, projected to the position of the observer, and it can be measured when the signature of the Earth’s orbit is seen in light curve (Muraki et al. 2011) or from observations from a telescope in a Heliocentric orbit (Udalski et al. 2015). For events with caustic crossings or planetary features, observations from Earth and L2 can also measure π_E (Wyrzykowski et al. 2020). However, both ground-based and space-based π_E measurements are susceptible to systematic photometry errors (Koshimoto & Bennett 2020; Koshimoto et al. 2021; Yee et al. 2021), so some care is required when interpreting the π_E values from light curve models.

The final method to determine a mass-distance relation is to measure the brightness of the planetary host star (which is also the lens star). For ground-based surveys, this can be accomplished with high angular resolution follow-up observations using the *Hubble Space Telescope* or a large ground-based telescope with a laser guide star adaptive optics system (e.g., Bennett et al. 2015; Batista et al. 2015). These high angular resolution observations are needed to resolve the lens star separating from the source star in order to avoid confusion with other nearby stars other than the lens (and planetary host) (Bhattacharya et al. 2017; Koshimoto et al. 2020). For a space-based exoplanet microlensing survey, like the one planned for *Roman*, the survey data have high enough angular resolution to detect the lens stars and measure the lens-source relative proper motion, $\boldsymbol{\mu}_{\text{rel}}$ (Bennett & Rhie 2002; Bennett et al. 2007). The measurement of $\boldsymbol{\mu}_{\text{rel}}$ is also useful for confirming the lens star identification since the length of the $\boldsymbol{\mu}_{\text{rel}}$ vector can be determined from light curve parameters, $\mu_{\text{rel}} = \theta_*/t_*$. In addition the $\boldsymbol{\mu}_{\text{rel}}$ and $\boldsymbol{\pi}_E$ vectors have the same direction, so a measurement of $\boldsymbol{\mu}_{\text{rel}}$ can be used to test for systematic errors in $\boldsymbol{\pi}_E$ measurements or to provide precise π_E measurements when the light curve only imposes a strong constraint on one component of $\boldsymbol{\pi}_E$ (Bhattacharya et al. 2018; Bennett et al. 2020).

We should also note that these three mass-distance relations are also useful for demographics studies even in cases where only one of the mass-distance constraints is measured precisely (Koshimoto et al. 2021). Of course, a single mass-distance constraint will produce a mass-distance degeneracy in the interpretation. However, a typical microlensing survey will have some events with mass measurements, and some with a combination of a single mass-distance relation with upper and/or lower bounds on the other mass-distance relation parameters. For microlensing event MOA-2010-BLG-477, a measurement of θ_E , upper and lower limits on π_E , and an upper limit on the host star brightness imply that the host of the gas giant planet is a white dwarf (Blackman et al. 2021).

6.2. Tier I Data Products

1. Stellar sample properties

- (a) List of all microlensing events in the sample including coordinates and measured t_E , t_0 , and u_0 values. When t_* is measured, it should be reported, too. For surveys including binary star host systems, the binary microlensing model parameters should also be included.

2. Survey properties

- (a) Description of detection thresholds for events included in sample (e.g., $\Delta\chi^2$ cuts)
- (b) Average detection efficiencies across the survey as a function of q , s , and t_E , or

- (c) Method for estimating source radius crossing time, t_* , or equivalently, the source size in Einstein radius units ($\rho = t_*/t_E$) for events without planetary signals or finite source effects. This is used for detection efficiency calculations.

3. Planet catalog properties

- (a) Observed properties of each microlensing event: mass ratio (q), projected separation (s , in Einstein radius units), angle between source trajectory and lens axis, α , and source magnitude in one or more passbands, with error bars. For events with finite source effects (most, but not all planetary events), also include the source radius crossing time, t_* . For events with detected multiple planet systems, the additional parameters needed to describe the event should also be included.
- (b) Mass-distance relation properties of each host star
- microlensing parallax, π_E , a two-dimensional vector, with error bars
 - angular Einstein radius, θ_E , usually calculated from finite source effects
 - host star brightness or limits in one or more passbands
 - relative lens-source proper motion, μ_{rel} , a two-dimensional vector, as measured from high angular resolution observations before or after the event
- (c) For events with degenerate models, include t_E , q , s , α , and t_* for all degenerate models with error bars; also include a weighting for each model, with the calculation method used to determine the weighting.

6.3. Tier II Data Products

1. Stellar sample properties

- (a) Distribution of host star and stellar remnant masses surveyed for planets and the Galactic model used to calculate this distribution.

2. Survey properties

- (a) **Planet detection efficiencies as a function of s and q for each microlensing event in the sample.** Ideally, this would extend upward through mass the mass ratios corresponding the brown dwarf and stellar mass secondaries, although most analyses to date have not done this. This enables the straight forward combination of multiple microlensing demographic analyses, and it is probably the most useful of the exoplanet microlensing demographics data products.

7. ASTROMETRY

Astrometry involves measuring the positions of celestial bodies. As such, it provides two-dimensional information—typically in the right ascension and declination axes—about objects that give information about trajectories on the sky (proper motions), as well as distances (parallaxes). In addition, astrometry yields information on the motions of bodies in gravitationally bound systems involving multiple objects, such as binary asteroids, moons orbiting planets, trans-Neptunian objects, and stars. Over the past few decades, astrometric capabilities have advanced to the point where detections of exoplanets orbiting other stars are within reach (Lurie et al. 2014; Boss et al.

2017; Kervella et al. 2022). This section describes data requirements for exoplanets orbiting other stars that are detected via astrometry.

The resulting astrometric signal maps the position of the combined light of the target system, which means in the case of an exoplanetary system the observed astrometric displacements represent only those of the host star. However, the same observational signal may be mimicked by a binary star in which the components have nearly equal fluxes. In that case, the system’s observed center of light is only slightly displaced from the system’s barycenter. Potential detections must therefore be examined with high resolution imaging techniques to rule out the possibility that a non-planetary mass luminous companion is causing the astrometric orbital signature.

The items below describe the minimum data products that should be provided for surveys of stars for exoplanet companions via astrometry, followed by additional recommended data products.

7.1. Tier I Data Products

1. Stellar sample properties

- (a) Number of stars in survey
- (b) Description of the stellar sample that was searched, including target selection criteria (RA/Dec, distance (preferably trigonometric parallax), absolute magnitude, photometric color)
- (c) Stellar masses and method by which those were determined. This property should already be known for at least every planet detection, as the stellar mass is necessary to distinguish if a signal is from a planetary companion or a stellar companion.

2. Survey properties

- (a) Survey facility information (telescope, including aperture; instrument, including pixel scale and filter(s) used)
- (b) Representative value of the number of observing epochs (nights/months/years) typical per target
- (c) For each target, the five-parameter astrometric solutions (position = RA+Dec, parallax, and proper motions in RA+Dec with uncertainties)
- (d) **Total survey duration, including start and end dates and representative value of the total years of observational coverage per target**
- (e) **Typical sensitivity per target in milliarcseconds at orbital periods of up to N years. This property essentially summarizes the implications of the survey properties listed above. Most surveys will be doing this already, on at least a target-by-target basis, as part of their search for potential planetary signals.**
- (f) For targets without detections, typical sensitivity in Jupiter masses at orbital periods up to N years (assuming stellar mass and various stated orbital parameters). This property may take some additional analysis to produce, but it is necessary for any comparisons with other results to be meaningful. It also indicates if the validity of these non-detections will need to be reassessed when any of the dependent properties (such as stellar mass, stellar multiplicity, or possible planet orbits) are later updated.

In particular, the above properties (a) through (d) should be well known for any survey target without additional effort.

3. Planet catalog properties

- (a) For each detection, the photocentric orbit parameters and their uncertainties, with a thorough description of the astrometric model, including how the following seven parameters are determined simultaneously with the five basic astrometry parameters:
- P = orbital period
 - a = semi-major axis
 - e = eccentricity
 - i = inclination
 - ω = argument of periastron
 - Ω = longitude of ascending node
 - T_o = epoch of periastron
 - equinox of the grid used to set angles

These orbital elements should also be reported in the form of the Thiele-Innes constants (A, B, F, and G).

These parameters should already be produced for every planet detection as part of the analysis to determine if the signal is from a planetary companion or a stellar companion.

- (b) For each detection, a figure showing the perturbations on each axis (RA vs. time and Dec vs. time) with respect to the astrometric model fit. The data behind these figures should also be made available in machine-readable format.
- (c) Some measure of the probability that a given signal is not explained by a 5-parameter single-object astrometric model. This is more appropriate for a large survey result, rather than a report of a planet (or planets) orbiting a given star.
- (d) Contrast curves from high-resolution imaging of the targets to eliminate the possibility that the astrometric signal is due to a luminous stellar or brown dwarf companion, rather than a planet. This data product should already be produced for every planet detection as part of that analysis.

7.2. Tier II Data Products

1. Stellar sample properties

For each target star:

- (a) Stellar luminosity and determination method
- (b) Stellar temperature and determination method

2. Survey properties

- (a) Total duration of observations on each individual target, including start and end dates and the total years of observational coverage
- (b) Number of observing epochs (nights/months/years) on each target

- (c) For each target, sensitivity in milliarcseconds at orbital periods of $1-N$ years, with values provided at key orbital periods within that range. This property will require some analysis of the residuals to the proper motion and parallax fits, but many surveys will likely be doing this already as part of their search for potential planetary signals.
- (d) For each target without detections, sensitivity in Jupiter masses at orbital periods of $1-N$ years (assuming stellar mass and various stated orbital parameters), with values provided at key orbital periods within that range. These curves should thus capture the mass limits of companions ruled out by the astrometric time series. This information can be concisely presented for each target in a single figure, for example as in Figure 4 of Lurie et al. (2014). Each such curve may take some additional analysis to produce, but it will enable meaningful comparisons with results covering different ranges of orbital period space. These curves also allow the validity of these non-detections to be reassessed on a target-by-target basis if any of their dependent properties (such as stellar mass, stellar multiplicity, or possible planet orbits) are later updated.
- (e) A periodogram of the astrometric residuals to the proper motion and parallax fits on each directional axis (RA and Dec).
- (f) Data frames that are flat-fielded and bias-subtracted, as well as plate constants specific to those frames.
- (g) Centroid positions in RA and Dec at each epoch for the target star and each reference star used in the analysis.

3. Planet catalog properties

- (a) For each detection, a figure showing the photocentric orbit in the plane of the sky (RA vs. Dec) with proper motion and parallax removed. This product will be helpful for comparing other results to this detection, in particular for audiences unaccustomed to astrometry data.
- (b) For non-detections, a figure showing the photocenter residuals after solving for parallax and proper motion on each axis (RA vs. time and Dec vs. time)

8. DATA ARCHIVING

The sections above have outlined the data products that the ExoPAG SIG on Exoplanet Demographics finds would be valuable when published alongside exoplanet survey data, in order to allow for the usage of those survey data by the wider exoplanet demographics community. However, one topic that we did not cover was the logistics of archiving these data such that they are reliably and permanently accessible. We recognize that some of the data products are non-trivial in size, and/or do not naturally conform to the data standards typically accommodated by journals. We also want to encourage authors to make their simulated data sets available where possible, which will incur additional overheads.

There are several archiving options that are already available to the community. The Direct Imaging Virtual Archive (DIVA)⁷ houses high-level science products (HSLPs) across multiple direct imaging

⁷ Direct Imaging Virtual Archive: <http://cesam.lam.fr/diva/>

detection surveys, providing an example of a repository for the kinds of data that are needed to perform demographics studies across surveys. In particular, DIVA encourages the use of a consistent format, HCI-FITS, for the uploading and storage of HLSPs, “to simplify HLSP exchange in the HCI community by adopting a standard output format for all the usual data products”. DIVA currently hosts nearly 20 GB of data across 16 direct imaging surveys, and invite other surveys to contribute data.

The NASA Exoplanet Archive hosts contributed datasets from the community⁸ and a substantial amount of ancillary survey data and HLSPs from the NASA *Kepler* mission, including detailed characterizations of the survey detection efficiency and reliability of the types described here^{9,10}. They also host a large number of transiting and radial velocity survey data sets, and are open to hosting additional data sets by request.

The VizieR Information Service¹¹, hosted by the Strasbourg astronomical Data Center (CDS), provides a standardized description of astronomical catalogues and access to the data therein. Large tables of data, such as stellar and planet catalog parameters, and injection/recovery results, are able to be hosted and accessed in a variety of ways.

The Mikulski Archive for Space Telescopes (MAST) hosts a wide-variety of community-created HLSPs¹². These HLSPs contain observations, catalogs, models or simulations that complement, or are derived from, MAST-supported missions. These missions include *Hubble*, *Webb*, *Kepler*, *TESS* and *Roman*.

In addition to the above options, there are also typically hosting options available at the authors’ home institutions, however there can be questions about the long-term storage and accessibility of these ad hoc sites. We encourage authors to find a permanent archival home for their data products, to ensure their ongoing accessibility and usage.

⁸ NASA Exoplanet Archive: Contributed Data Sets: https://exoplanetarchive.ipac.caltech.edu/docs/contributed_data.html

⁹ Kepler Completeness and Reliability Products: https://exoplanetarchive.ipac.caltech.edu/docs/Kepler_completeness_reliability.html

¹⁰ Kepler Simulated Data Products: <https://exoplanetarchive.ipac.caltech.edu/docs/KeplerSimulated.html>

¹¹ ViZieR: <https://vizier.u-strasbg.fr/viz-bin/VizieR>

¹² MAST HLSPs: <https://archive.stsci.edu/hlsp/>

REFERENCES

- Baraffe, I., Chabrier, G., Barman, T. S., Allard, F., & Hauschildt, P. H. 2003, *A&A*, 402, 701, doi: [10.1051/0004-6361:20030252](https://doi.org/10.1051/0004-6361:20030252)
- Batista, V., Beaulieu, J.-P., Bennett, D. P., et al. 2015, *ApJ*, 808, 170, doi: [10.1088/0004-637X/808/2/170](https://doi.org/10.1088/0004-637X/808/2/170)
- Bennett, D. P., Anderson, J., & Gaudi, B. S. 2007, *ApJ*, 660, 781, doi: [10.1086/513013](https://doi.org/10.1086/513013)
- Bennett, D. P., & Rhie, S. H. 1996, *ApJ*, 472, 660, doi: [10.1086/178096](https://doi.org/10.1086/178096)
- . 2002, *ApJ*, 574, 985, doi: [10.1086/340977](https://doi.org/10.1086/340977)
- Bennett, D. P., Bhattacharya, A., Anderson, J., et al. 2015, *ApJ*, 808, 169, doi: [10.1088/0004-637X/808/2/169](https://doi.org/10.1088/0004-637X/808/2/169)
- Bennett, D. P., Bhattacharya, A., Beaulieu, J.-P., et al. 2020, *AJ*, 159, 68, doi: [10.3847/1538-3881/ab6212](https://doi.org/10.3847/1538-3881/ab6212)
- Beuzit, J. L., Vigan, A., Mouillet, D., et al. 2019, *A&A*, 631, A155, doi: [10.1051/0004-6361/201935251](https://doi.org/10.1051/0004-6361/201935251)
- Bhattacharya, A., Bennett, D. P., Anderson, J., et al. 2017, *AJ*, 154, 59, doi: [10.3847/1538-3881/aa7b80](https://doi.org/10.3847/1538-3881/aa7b80)
- Bhattacharya, A., Beaulieu, J. P., Bennett, D. P., et al. 2018, *AJ*, 156, 289, doi: [10.3847/1538-3881/aaed46](https://doi.org/10.3847/1538-3881/aaed46)
- Blackman, J. W., Beaulieu, J. P., Bennett, D. P., et al. 2021, *Nature*, 598, 272, doi: [10.1038/s41586-021-03869-6](https://doi.org/10.1038/s41586-021-03869-6)
- Borucki, W. J., & Summers, A. L. 1984, *Icarus*, 58, 121, doi: [10.1016/0019-1035\(84\)90102-7](https://doi.org/10.1016/0019-1035(84)90102-7)
- Boss, A. P., Weinberger, A. J., Keiser, S. A., et al. 2017, *AJ*, 154, 103, doi: [10.3847/1538-3881/aa84b5](https://doi.org/10.3847/1538-3881/aa84b5)
- Bowler, B. P. 2016, *PASP*, 128, 102001, doi: [10.1088/1538-3873/128/968/102001](https://doi.org/10.1088/1538-3873/128/968/102001)
- Cassan, A., Kubas, D., Beaulieu, J.-P., et al. 2012, *Nature*, 481, 167, doi: [10.1038/nature10684](https://doi.org/10.1038/nature10684)
- Christiansen, J. L., Clarke, B. D., Burke, C. J., et al. 2020, *AJ*, 160, 159, doi: [10.3847/1538-3881/abab0b](https://doi.org/10.3847/1538-3881/abab0b)
- Clanton, C., & Gaudi, B. S. 2014, *ApJ*, 791, 91, doi: [10.1088/0004-637X/791/2/91](https://doi.org/10.1088/0004-637X/791/2/91)
- . 2016, *ApJ*, 819, 125, doi: [10.3847/0004-637X/819/2/125](https://doi.org/10.3847/0004-637X/819/2/125)
- Dawson, R. I., & Murray-Clay, R. A. 2013, *ApJL*, 767, L24, doi: [10.1088/2041-8205/767/2/L24](https://doi.org/10.1088/2041-8205/767/2/L24)
- Fernandes, R. B., Mulders, G. D., Pascucci, I., Mordasini, C., & Emsenhuber, A. 2019, *ApJ*, 874, 81, doi: [10.3847/1538-4357/ab0300](https://doi.org/10.3847/1538-4357/ab0300)
- Fulton, B. J., Rosenthal, L. J., Hirsch, L. A., et al. 2021, *ApJS*, 255, 14, doi: [10.3847/1538-4365/abfcc1](https://doi.org/10.3847/1538-4365/abfcc1)
- Gagné, J., & Faherty, J. K. 2018, *ApJ*, 862, 138, doi: [10.3847/1538-4357/aaca2e](https://doi.org/10.3847/1538-4357/aaca2e)
- Gaudi, B. S. 2012, *ARA&A*, 50, 411, doi: [10.1146/annurev-astro-081811-125518](https://doi.org/10.1146/annurev-astro-081811-125518)
- Gaudi, B. S., Albrow, M. D., An, J., et al. 2002, *ApJ*, 566, 463, doi: [10.1086/337987](https://doi.org/10.1086/337987)
- Ginzburg, S., Schlichting, H. E., & Sari, R. 2018, *MNRAS*, 476, 759, doi: [10.1093/mnras/sty290](https://doi.org/10.1093/mnras/sty290)
- Gould, A., & Loeb, A. 1992, *ApJ*, 396, 104, doi: [10.1086/171700](https://doi.org/10.1086/171700)
- Gould, A., Dong, S., Gaudi, B. S., et al. 2010, *ApJ*, 720, 1073, doi: [10.1088/0004-637X/720/2/1073](https://doi.org/10.1088/0004-637X/720/2/1073)
- He, M. Y., Ford, E. B., & Ragozzine, D. 2019, *MNRAS*, 490, 4575, doi: [10.1093/mnras/stz2869](https://doi.org/10.1093/mnras/stz2869)
- Howard, A. W., Marcy, G. W., Bryson, S. T., et al. 2012, *ApJS*, 201, 15, doi: [10.1088/0067-0049/201/2/15](https://doi.org/10.1088/0067-0049/201/2/15)
- Hsu, D. C., Ford, E. B., Ragozzine, D., & Ashby, K. 2019, arXiv e-prints, arXiv:1902.01417. <https://arxiv.org/abs/1902.01417>
- Jehin, E., Gillon, M., Queloz, D., et al. 2011, *The Messenger*, 145, 2
- Jin, S., & Mordasini, C. 2018, *ApJ*, 853, 163, doi: [10.3847/1538-4357/aa9f1e](https://doi.org/10.3847/1538-4357/aa9f1e)
- Kervella, P., Arenou, F., & Thévenin, F. 2022, *A&A*, 657, A7, doi: [10.1051/0004-6361/202142146](https://doi.org/10.1051/0004-6361/202142146)
- Koshimoto, N., & Bennett, D. P. 2020, *AJ*, 160, 177, doi: [10.3847/1538-3881/abaf4e](https://doi.org/10.3847/1538-3881/abaf4e)
- Koshimoto, N., Bennett, D. P., & Suzuki, D. 2020, *AJ*, 159, 268, doi: [10.3847/1538-3881/ab8adf](https://doi.org/10.3847/1538-3881/ab8adf)
- Koshimoto, N., Bennett, D. P., Suzuki, D., & Bond, I. A. 2021, *ApJL*, 918, L8, doi: [10.3847/2041-8213/ac17ec](https://doi.org/10.3847/2041-8213/ac17ec)
- Kunimoto, M., & Bryson, S. 2021, *AJ*, 161, 69, doi: [10.3847/1538-3881/abd2c1](https://doi.org/10.3847/1538-3881/abd2c1)
- Kunimoto, M., Huang, C., Tey, E., et al. 2021a, *Research Notes of the American Astronomical Society*, 5, 234, doi: [10.3847/2515-5172/ac2ef0](https://doi.org/10.3847/2515-5172/ac2ef0)

- Kunimoto, M., Daylan, T., Guerrero, N., et al. 2021b, arXiv e-prints, arXiv:2112.02176.
<https://arxiv.org/abs/2112.02176>
- Lee, E. J., & Chiang, E. 2016, *ApJ*, 817, 90,
 doi: [10.3847/0004-637X/817/2/90](https://doi.org/10.3847/0004-637X/817/2/90)
- Lurie, J. C., Henry, T. J., Jao, W.-C., et al. 2014, *AJ*, 148, 91, doi: [10.1088/0004-6256/148/5/91](https://doi.org/10.1088/0004-6256/148/5/91)
- Macintosh, B., Chilcote, J. K., Bailey, V. P., et al. 2018, in *Society of Photo-Optical Instrumentation Engineers (SPIE) Conference Series*, Vol. 10703, *Adaptive Optics Systems VI*, ed. L. M. Close, L. Schreiber, & D. Schmidt, 107030K, doi: [10.1117/12.2314253](https://doi.org/10.1117/12.2314253)
- Marley, M. S., Saumon, D., Visscher, C., et al. 2021, *ApJ*, 920, 85,
 doi: [10.3847/1538-4357/ac141d](https://doi.org/10.3847/1538-4357/ac141d)
- Mordasini, C., van Boekel, R., Mollière, P., Henning, T., & Benneke, B. 2016, *ApJ*, 832, 41,
 doi: [10.3847/0004-637X/832/1/41](https://doi.org/10.3847/0004-637X/832/1/41)
- Mulders, G. D., Pascucci, I., & Apai, D. 2015, *ApJ*, 798, 112,
 doi: [10.1088/0004-637X/798/2/112](https://doi.org/10.1088/0004-637X/798/2/112)
- Mulders, G. D., Pascucci, I., Apai, D., & Ciesla, F. J. 2018, *AJ*, 156, 24,
 doi: [10.3847/1538-3881/aac5ea](https://doi.org/10.3847/1538-3881/aac5ea)
- Muraki, Y., Han, C., Bennett, D. P., et al. 2011, *ApJ*, 741, 22, doi: [10.1088/0004-637X/741/1/22](https://doi.org/10.1088/0004-637X/741/1/22)
- Nielsen, E. L., De Rosa, R. J., Macintosh, B., et al. 2019, *AJ*, 158, 13,
 doi: [10.3847/1538-3881/ab16e9](https://doi.org/10.3847/1538-3881/ab16e9)
- Nucita, A. A., Licchelli, D., De Paolis, F., et al. 2018, *MNRAS*, 476, 2962,
 doi: [10.1093/mnras/sty448](https://doi.org/10.1093/mnras/sty448)
- Nutzman, P., & Charbonneau, D. 2008, *PASP*, 120, 317, doi: [10.1086/533420](https://doi.org/10.1086/533420)
- Owen, J. E., & Wu, Y. 2017, *ApJ*, 847, 29,
 doi: [10.3847/1538-4357/aa890a](https://doi.org/10.3847/1538-4357/aa890a)
- Pascucci, I., Mulders, G. D., Gould, A., & Fernandes, R. 2018, *The Astrophysical Journal Letters*, 856, L28
- Pascucci, I., Mulders, G. D., Gould, A., & Fernandes, R. 2018, *ApJL*, 856, L28,
 doi: [10.3847/2041-8213/aab6ac](https://doi.org/10.3847/2041-8213/aab6ac)
- Penny, M. T., Gaudi, B. S., Kerins, E., et al. 2019, *ApJS*, 241, 3, doi: [10.3847/1538-4365/aafb69](https://doi.org/10.3847/1538-4365/aafb69)
- Poleski, R., Skowron, J., Mróz, P., et al. 2021, arXiv e-prints, arXiv:2104.02079.
<https://arxiv.org/abs/2104.02079>
- Ricker, G. R., Winn, J. N., Vanderspek, R., et al. 2015, *Journal of Astronomical Telescopes, Instruments, and Systems*, 1, 014003,
 doi: [10.1117/1.JATIS.1.1.014003](https://doi.org/10.1117/1.JATIS.1.1.014003)
- Rosenthal, L. J., Fulton, B. J., Hirsch, L. A., et al. 2021, *ApJS*, 255, 8,
 doi: [10.3847/1538-4365/abe23c](https://doi.org/10.3847/1538-4365/abe23c)
- Sumi, T., Bennett, D. P., Bond, I. A., et al. 2010, *ApJ*, 710, 1641,
 doi: [10.1088/0004-637X/710/2/1641](https://doi.org/10.1088/0004-637X/710/2/1641)
- Suzuki, D., Bennett, D. P., Sumi, T., et al. 2016, *ApJ*, 833, 145,
 doi: [10.3847/1538-4357/833/2/145](https://doi.org/10.3847/1538-4357/833/2/145)
- Thompson, S. E., Coughlin, J. L., Hoffman, K., et al. 2018, *ApJS*, 235, 38,
 doi: [10.3847/1538-4365/aab4f9](https://doi.org/10.3847/1538-4365/aab4f9)
- Udalski, A., Yee, J. C., Gould, A., et al. 2015, *ApJ*, 799, 237,
 doi: [10.1088/0004-637X/799/2/237](https://doi.org/10.1088/0004-637X/799/2/237)
- Vigan, A., Fontanive, C., Meyer, M., et al. 2021, *A&A*, 651, A72,
 doi: [10.1051/0004-6361/202038107](https://doi.org/10.1051/0004-6361/202038107)
- Wolfgang, A., Rogers, L. A., & Ford, E. B. 2016, *ApJ*, 825, 19, doi: [10.3847/0004-637X/825/1/19](https://doi.org/10.3847/0004-637X/825/1/19)
- Wyrzykowski, L., Mróz, P., Rybicki, K. A., et al. 2020, *A&A*, 633, A98,
 doi: [10.1051/0004-6361/201935097](https://doi.org/10.1051/0004-6361/201935097)
- Yee, J. C., Gould, A., Beichman, C., et al. 2015, *ApJ*, 810, 155,
 doi: [10.1088/0004-637X/810/2/155](https://doi.org/10.1088/0004-637X/810/2/155)
- Yee, J. C., Zang, W., Udalski, A., et al. 2021, *AJ*, 162, 180, doi: [10.3847/1538-3881/ac1582](https://doi.org/10.3847/1538-3881/ac1582)
- Yu, H., Weinberg, N. N., & Arras, P. 2021, *ApJ*, 917, 31, doi: [10.3847/1538-4357/ac0a79](https://doi.org/10.3847/1538-4357/ac0a79)
- Zink, J. K., & Hansen, B. M. S. 2019, *MNRAS*, 1201, doi: [10.1093/mnras/stz1246](https://doi.org/10.1093/mnras/stz1246)
- Zink, J. K., Hardegree-Ullman, K. K., Christiansen, J. L., et al. 2021, arXiv e-prints, arXiv:2109.02675.
<https://arxiv.org/abs/2109.02675>

The authors would like to gratefully acknowledge those members of the community who provided feedback on initial drafts of this report. These include Eric Ford, Timothy Brandt, Andreas Quirrenbach, Jonathan Zink, Michelle Kunimoto, and Eric Mamajek. Thank you for your careful attention and helpful suggestions!